

Minimally Parametric Constraints on the Primordial Power Spectrum from Lyman-alpha

Simeon Bird

Institute of Astronomy and Kavli Institute for Cosmology, University of Cambridge, Cambridge, UK

Current analyses of the Lyman-alpha forest assume that the primordial power spectrum of density perturbations obeys a simple power law, a strong theoretical assumption which should be tested. Employing a large suite of numerical simulations which drop this assumption, we reconstruct the shape of the primordial power spectrum using Lyman-alpha data from the Sloan Digital Sky Survey (SDSS). Our method combines a minimally parametric framework with cross-validation, a technique used to avoid over-fitting the data. Future work will involve predictions for the upcoming Baryon Oscillation Sky Survey (BOSS), which will provide new Lyman-alpha data with vastly decreased statistical errors.

1 Introduction

The Lyman- α forest is the name given to a series of absorption lines in quasar spectra, caused by the scattering of photons via interaction with neutral hydrogen at redshifts 2 – 4. At these redshifts, a large proportion of the baryon density of the universe is contained within hydrogen clouds. Most of the hydrogen is ionized, but a small fraction remains neutral, and absorbs photons via the Lyman- α transition. Hence, the Lyman- α forest is sensitive to the matter power spectrum on scales from a few up to tens of Mpc, making it the only currently available probe of fluctuations at these weakly non-linear scales. A number of authors have examined the constraints obtainable from the Lyman- α forest in the past, including Croft et al¹, Gnedin & Hamilton², Viel, Haehnelt & Springel³.

Previous analyses of constraints from the Lyman- α forest have assumed that the primordial power spectrum is described by a nearly scale-invariant power law. This deserves further attention for a number of reasons. First, it is a strong assumption; if the data are inconsistent with it, derived constraints could be biased to some extent. Second, it is a generic prediction of inflationary models; hence, any test of a power law primordial power spectrum which cannot be attributed to data systematics is a test of inflation. Third, of all current datasets, the Lyman- α constrains the smallest cosmological scales; thus, it provides the best opportunity presently available to understand the overall shape of the power spectrum. To do this, we shall reconstruct the primordial power spectrum in a minimally parametric way, using a technique called cross-validation to robustly recover the signal. If the data are in agreement with theoretical expectations, the recovered power spectrum will be nearly scale-invariant. In these Proceedings, we discuss a minimally parametric framework for constraining the primordial matter power spectrum, the cross-validation technique, and the methodology for obtaining constraints from observations. Finally, some preliminary results are presented.

2 Flux Power Spectrum

In the case of Lyman- α , the observable is not a direct measurement of the clustering properties of tracer objects, as in galaxy clustering, but the statistics of absorption along a number of quasar sightlines. It is easiest to work with the statistics of the flux, \mathcal{F} , defined as

$$\mathcal{F} = \exp(-\tau), \quad (1)$$

where τ is the optical depth. The primary observable here is the one dimensional flux power spectrum, P_F ,

$$P_F(k) = |\tilde{\mathcal{F}}(k)|^2, \quad (2)$$

where $\tilde{\mathcal{F}}$ is the Fourier transform of the flux, evaluated as a function of distance along the line of sight,

$$\tilde{\mathcal{F}}(k) = \int \mathcal{F}(x) e^{ikx} dx. \quad (3)$$

Current constraints on P_F are given by McDonald et al⁴, determined from ~ 3000 SDSS quasar spectra.

In order to simulate the observable flux power spectrum from a given set of primordial fluctuations, a large N -body simulation is required. This makes it impractical to directly calculate P_F for every possible set of input parameters; instead simulations are run for a representative sample. Other results are obtained via interpolation, using the following scheme of Viel & Haehnelt⁵. The flux power spectrum is assumed to be given by a Taylor expansion around some best-fit model. For a vector of parameters p_i , with best-fit model parameters p_i^0 , the flux power spectrum P_F is given by

$$P_F(p_i) = P_F(p_i^0) + \Sigma_i (p_i - p_i^0) \frac{\partial P_F}{\partial p_i} + \Sigma_i (p_i - p_i^0)^2 \frac{\partial^2 P_F}{\partial p_i^2}. \quad (4)$$

Numerical simulations are used to calculate the derivatives of the flux power spectrum. Each parameter is varied independently, and the total change in the flux power spectrum is assumed to be a linear combination of the change due to each parameter, i.e.,

$$\delta P_F = \frac{\delta P_F}{\delta p_1} \delta p_1 + \frac{\delta P_F}{\delta p_2} \delta p_2 + \dots \quad (5)$$

Figure 1 shows the error due to this approximation for a sample input primordial power spectrum. The error is around 1% on scales probed by current Lyman- α data ($k = 0.4 - 2 \text{ h Mpc}^{-1}$), which is a small contribution to the total error, allowing us to proceed with confidence. Further checks on interpolation errors are in progress, and are expected to give similar results.

3 Power Spectrum Reconstruction

Previous analyses of the Lyman- α forest^{3,8} have assumed the primordial power spectrum is a nearly scale-invariant power law, of the form

$$P(k) = A_s \left(\frac{k}{k_0} \right)^{n_s-1}. \quad (6)$$

As discussed above, we seek to test whether the data supports this assumption by reconstructing the power spectrum with smoothing splines^a, as proposed in Sealfon et al⁶. Smoothing splines

^aSplines are piecewise cubic polynomials with globally continuous first and second derivatives, completely specified by their values at a series of knots, where the polynomials meet.

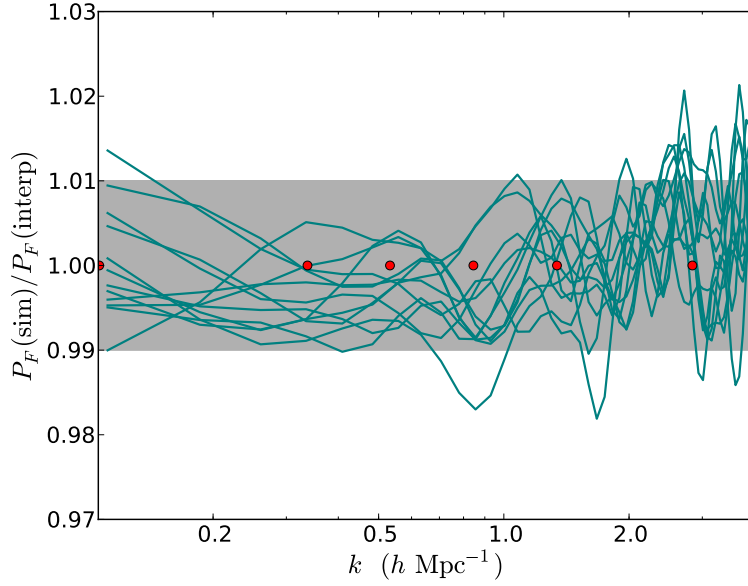


Figure 1: The difference between the flux power spectrum as obtained from interpolation, using Eq. 4, and directly by simulation. Each line represents simulation output at a different redshift bin, between $z = 2.0$ and $z = 4.2$. Red dots show the positions of spline knots. The grey band shows 1% error bars.

are used because they have good continuity properties and are particularly suited to formulation of a cross-validation penalty.

4 Cross-Validation

Any minimally parametric formalism, when applied to noisy data, runs the risk of over-fitting the data. One way to avoid this problem is a technique called cross-validation, described in Peiris & Verde⁷. This technique assumes that noise in the data takes the form of additional small-scale structure, and thus power spectra with superfluous fluctuations should be penalised. This penalty is implemented by adding an extra term to the likelihood function, \mathcal{L} ;

$$\log \mathcal{L} = \log \mathcal{L}(\text{Data}|P(k)) + \lambda \int_k dk (P''(k))^2. \quad (7)$$

Here λ , the penalty weight, is a free parameter. In the limit $\lambda \rightarrow \infty$ this likelihood becomes functionally identical to linear regression, while $\lambda \rightarrow 0$ is appropriate in the case of noiseless data. In order to determine the optimal value for λ , the data points are first divided into two sets, the training set, or CV1, and the validation set, or CV2. CV1 and CV2 are composed of alternating data bins. Next, to calculate the CV score, a value is chosen for λ , and the best fit power spectrum based on the CV1 dataset is found. The χ^2 is then calculated for this power spectrum with the CV2 dataset. This is repeated, replacing CV1 with CV2 and vice versa, and the CV score is the sum of both χ^2 values.

The key to cross-validation is that signal in the CV1 dataset will predict signal in the CV2 dataset well, while noise in CV1 will predict noise in CV2 poorly. The optimal choice of λ is therefore the one which allows maximal predictivity between CV1 and CV2; in other words, minimizes the CV score.

5 Results

We performed a large grid of N -body simulations using Gadget-II⁹. Convergence checks were carried out to ensure P_F was not significantly affected by simulation settings¹⁰, such as particle resolution or box size. Initial conditions included a variety of input power spectra, on scales ranging from $k = 0.45 - 2 h \text{ Mpc}^{-1}$.

A significant departure from a power law primordial power spectrum translates to a detectable feature in the flux power spectrum, which is more noticeable at higher redshifts. This is due to the way in which the matter power spectrum evolves: a feature in the matter power spectrum will create extra non-linear growth on smaller scales, making the feature in P_F stand out less. The results of the simulations provide a mapping between primordial and flux power spectra, which in turn provides a likelihood function for any given primordial power spectrum from SDSS data. The full data analysis, including cross-validation, is currently being carried out.

6 Future Prospects

The best constraints on the flux power spectrum currently come from the Sloan Digital Sky Survey (SDSS⁴), which contains ~ 3000 quasar sightlines. In the near future, better constraints will be available from the Baryon Acoustic Oscillation Sky Survey (BOSS¹¹), part of SDSS-III. This will contain 160000 quasar spectra between redshifts of 2.2 and 3, and should further increase the statistical power of the Lyman- α forest. We plan to make forecasts for BOSS in forthcoming work¹².

7 Acknowledgements

I thank my collaborators in this work, Hiranya Peiris, Matteo Viel and Licia Verde, for useful discussions. I am supported by STFC and by Pembroke College Cambridge. This work was performed using the Darwin Supercomputer of the University of Cambridge High Performance Computing Service (<http://www.hpc.cam.ac.uk/>), provided by Dell Inc. using Strategic Research Infrastructure Funding from the Higher Education Funding Council for England.

References

1. Croft R.A.C., Weinberg D. H., Bolte M., Burles S., Hernquist L., Katz N., Kirkman D., Tytler D., 2002, ApJ, 581, 20
2. Gnedin N.Y., Hamilton A.J.S., 2002, MNRAS, 334, 107
3. Viel M., Haehnelt M.G., Springel V., 2004, MNRAS, 354, 684
4. McDonald P., Seljak U., Burles S., et al, 2006, Ap. J. Suppl., 163, 80-109
5. Viel M., Haehnelt M.G., 2006, MNRAS, 365, 231-244
6. Sealton C., Verde L., Jimenez R., 2005, PRD 72, 103520
7. Peiris H., Verde L., 2008, JCAP 0807:009
8. McDonald P., Seljak U., Cen R., Shih D. et al, Ap.J. 635 761-78
9. Springel V., 2005, MNRAS, 364 1105-1134, astro-ph/0505010
10. Heitmann K., White M., Wagner C., Habib S., Higdon D, 2010, Ap.J 715, 104-121
11. SDSS collaboration, see Sec. 3 of <http://www.sdss3.org/collaboration/description.pdf>
12. Bird S., Peiris H., Viel M., Verde L., in preparation